Journal of Orthopaedic Translation (2016) 6, 1—9

Available online at www.sciencedirect.com

ScienceDirect

journal homepage: http://ees.elsevier.com/jot

ORIGINAL ARTICLE

In vivo magnetic resonance imaging features of spinal muscles in the ovine model

Stephanie Valentin [a,*], **Theresia Licka** [a,b], **Annika Essigbeck** [a], **James Elliott** [c,d]

[a] *Equine Clinic, University of Veterinary Medicine Vienna, Vienna, Austria*
[b] *Large Animal Hospital, Royal (Dick) School of Veterinary Studies, University of Edinburgh, Roslin, Scotland, United Kingdom*
[c] *Department of Physical Therapy and Human Movement Sciences, Feinberg School of Medicine, Northwestern University, Chicago, IL, USA*
[d] *School of Health and Rehabilitation Sciences, University of Queensland, Brisbane, Queensland, Australia*

Received 19 December 2014; received in revised form 28 August 2015; accepted 10 September 2015
Available online 23 October 2015

KEYWORDS
animal models;
lumbar spine;
magnetic resonance imaging;
muscle fatty infiltration;
ovine

Summary *Background:* Muscle fatty infiltration (MFI) has been identified in patients with spinal pain using magnetic resonance imaging (MRI). Even though sheep are a commonly used animal model for the human spine, comparative sheep MFI data from MRI is not available. Determining MFI in sheep spinal muscles using acquisition protocols commonly used in man will identify the applicability of this approach in future sheep model studies, such that the effects of spinal interventions on muscle can be assessed prior to their use in a human (clinical) population.
Objective: To quantify ovine lumbar spine MFI using three-dimensional two-point Dixon and T1-weighted sequences.
Methods: T1-weighted and Dixon lumbar spine axial sequences were collected in 14 healthy Austrian mountain sheep using a 1.5-T MRI. At each vertebrae, the region of interest of psoas major and minor (PS), multifidus (M), and longissimus (L) were identified. To determine MFI from the T1-weighted images, the mean pixel intensity (MPI) was calculated as a percentage of subcutaneous or intermuscular fat. For the Dixon images, fat sequence MPI was calculated as a percentage of the summed fat and water sequence MPIs. Spinal degeneration was graded and correlated to MFI. Dixon MFI was compared to T1-weighted MFI obtained from subcutaneous and intermuscular fat.
Results: For every muscle, T1-weighted MFI calculated using subcutaneous fat scored significantly lower than Dixon MFI and T1-weighted MFI calculated using intermuscular fat ($p < 0.001$). There were no significant MFI differences between T1-weighted images calculated using intermuscular fat and Dixon images for M and L ($p > 0.05$), although significant differences were found for PS.
Conclusion: In sheep, Dixon sequences provide an acceptable comparison to T1-weighted sequences for lumbar extensor MFI based on intermuscular fat. However, compared to the human

* Corresponding author. Equine Clinic, University of Veterinary Medicine Vienna, Veterinaerplatz 1, 1210 Wien, Austria.
E-mail address: stephanie.valentin@vetmeduni.ac.at (S. Valentin).

http://dx.doi.org/10.1016/j.jot.2015.09.004

literature, ovine lumbar musculature contains greater MFI, making interspecies comparisons more complex.

Introduction

Magnetic resonance imaging (MRI) is considered the imaging gold standard for quantifying muscle fatty infiltrate (MFI) [1]. Muscle composition has often been evaluated in patients with low back pain [2—6] and neck pain [7—11], as an increase in MFI in spinal muscles can been seen in these patients. Although T1-weighted images have been found reliable for MFI quantification in healthy females without neck pain [12], there are several more rapid imaging sequences that can be used to quantify [13] and correlate MFI with histology [1,14,15]. Sequences such as the Dixon method, where MFI data are collected when water and fat are in- and opposed-phase, have been used in healthy controls [16] and in patients with low back pain [17]. It has also been shown to be comparable to MFI obtained from T1-weighted imaging in the cervical multifidus in healthy adults [16].

The ovine is frequently used as an animal model for the investigation of spinal disorders and surgical interventions because of similarities in the *Homo sapiens* skeletal anatomy [18,19]. *In vivo* ovine studies investigating spinal implants are primarily performed to collect *in vitro* data on implant stability after the implant has been *in situ*, although other relevant *in vivo* data are not available [20]. Owing to the importance of the muscular system in spinal health [21,22], obtaining *in vivo* muscle parameters from animal models would be important to determine the validity of translational research between ovine and man. Although the amount of intramuscular fat in the ovine longissimus dorsi muscle has been published previously [23], these data were obtained at slaughter. To our knowledge, MFI in ovine spinal musculature has not been reported or compared to MRI quantification methods used in humans. Therefore, the aim of this study was to quantify and compare MFI in the ovine lumbar spine musculature using a T1-weighted and three-dimensional two-point Dixon sequence, as these sequences are commonly used to quantify muscle fat in humans. Additionally, two locations for fat calculation from the T1-weighted sequences were evaluated, as both methods have been used in previously published research [12,24].

Materials and methods

Study population

Seventeen healthy male and female Austrian mountain sheep were included in the study. A range of young and older sheep were included in order to identify the effect of age on MFI. The female sheep underwent an ultrasound investigation to exclude pregnancy. All sheep were assessed by an experienced orthopaedic veterinarian and were deemed medically fit to undergo anaesthesia for the imaging procedure of computed tomography (CT) and MRI. Ethical approval was obtained from the Austrian Federal Ministry of Science and Research (13/10/97/2011), and the guidelines for animal care and use were followed.

Data collection

Latero-lateral radiographs (Computed Radiography, Imaging plate Fuji) of the thoracic and lumbar spine were obtained (70 kV, 2.1 mAs; Super 100 CP; Philips, Eindhoven, The Netherlands) in unsedated sheep to identify the presence of any spinal pathology.

Prior to MRI, CT (Siemens Somatom Emotion 16; Siemens, Erlangen, Germany) was performed to ensure that the sheep did not have any metal in their bodies (i.e., ingested foreign objects) that could move when introduced to the magnetic field environment. The sheep were anaesthetised and placed in dorsal recumbency for CT and MRI data collection. Premedication for anaesthesia consisted of intravenous butorphanol (0.1 mg/kg) and xylazine (0.15 mg/kg). After obvious sedation was achieved, general anaesthesia was induced with ketamine (5 mg/mL) and maintained with inhalation of vaporised sevoflurane. For CT, dorsoventral images (80 kV, 25 mA, tilt 0.0, inversion time (TI) 10.6 seconds, slice thickness 0.6 mm, Display Field of View (DFOV) 153.3 cm × 153.3 cm) were obtained to determine the number of lumbar vertebrae and identify any potential foreign objects, and transverse images (130 kV, 200 mA, tilt 0.0 m TI 1.0 seconds, slice thickness 1.2 mm, DFOV 25.0 cm × 25.0 cm) were obtained to assess the presence of spinal pathology. For MRI data collection, lumbar spine T1-weighted and Dixon sequences were collected using a 1.5-T MRI (Siemens Magnetom Esprit; Siemens). T1-weighted images were obtained using a 4-mm slice thickness, 2-mm gap space, DFOV 450 mm × 450 mm, repetition time (TR) 448 ms, and echo time (TE) 11 ms. Dixon images were obtained using a 1.5-mm slice thickness, 1—5 mm gap space, DFOV 450 × 450 mm, TR 7.2 ms, TE 2.4 ms (oppose-phase), and TE 4.8 (in-phase). Axial images of the entire lumbar spine were obtained in up to three acquisitions. Attempts were made to obtain the entire lumbar spine in one acquisition, but in some sheep this was not possible owing to a risk of temperature increase because of a proportionally large fluid-filled rumen. In these cases, the lumbar spine was imaged in either two acquisitions (cranial and caudal lumbar spine) or in three acquisitions (cranial, middle, and caudal lumbar spine). A ventral to dorsal phase direction was used, and where this

was not possible because of substantial movement artefacts, sequences were run in a left to right phase direction.

At the end of the imaging procedure, sheep were placed in lateral recumbency until they showed active breathing movements, at which time they were extubated and the orogastric tube was removed. After extubation, sheep were placed in sternal recumbency in a clean stall with shavings and were continuously observed until they were stable at walk and stance.

Data analysis

For each lumbar vertebral body, an axial image closest in location to the mid vertebral body (based on absence of intervertebral discs or endplates and the transverse processes being well demarcated) was selected from the T1-weighted images. Dixon axial images which most closely matched the selected T1-weighted images were then selected. The last lumbar vertebra was defined as L6, regardless of whether sheep had six or seven lumbar vertebrae. The last investigated lumbar vertebra in all sheep was defined as L1, even though in sheep with seven lumbar vertebrae this would have been L2. From each axial T1-weighted and opposed-phase Dixon image, one assessor (SV) traced the region of interest (ROI) around the left and right sides of psoas major and minor (PS), multifidus (M), and longissimus (L; Figure 1) using the AnalyzeDirect software (version 11.0, Mayo Clinic, Rochester MN, USA). For the Dixon images, the in-phase ROIs were directly applied to the opposed-phase images. For the T1-weighted images, mean pixel intensity (MPI) was obtained from each ROI, and the average MPI from the left and right sides of each muscle per vertebral level was calculated. An ROI of intermuscular fat between PS and L from the left and right sides, and an ROI of subcutaneous fat from the right side of the body as close to the midline as possible were taken (Figure 2), and the MPI was calculated for these ROIs. An axial image from the last lumbar vertebrae where fat was most visible was chosen for these measures. T1-weighted MFI was determined relative to intermuscular fat and to subcutaneous fat by dividing the muscle MPI by that of the subcutaneous or intermuscular fat, and multiplying by 100 to obtain a percentage. To determine fat from the Dixon images, MPI from the fat sequence was divided by the summed fat and water MPI and multiplied by 100 to obtain a percentage.

For intrarater reliability, the ROI of the investigated muscles at each vertebral level in all sheep was traced a second time by the same assessor for the T1-weighted images and the cross-sectional areas (CSA) compared to the first assessment. For the second assessment, the assessor was blinded to the results from the first assessment.

To quantify pathological changes in the lumbar spine on CT, a grading system similar to that used in the canine species [25] was applied. Grading was performed by two assessors (AE and TL) by evaluation of the radiographs and CT images. Decisions were based on consensus opinion. At each vertebral level of the lumbar spine, degenerative changes were graded as follows: 0 = no pathological changes; 1 = minimal pathological changes (i.e., small osteophytes); 2 = moderate pathological changes present (i.e., large osteophytes without fusion to adjacent vertebra); and 3 = considerable pathological changes (i.e., large osteophytes creating a fusion with adjacent vertebra). For each sheep, the highest pathological grade observed was reported.

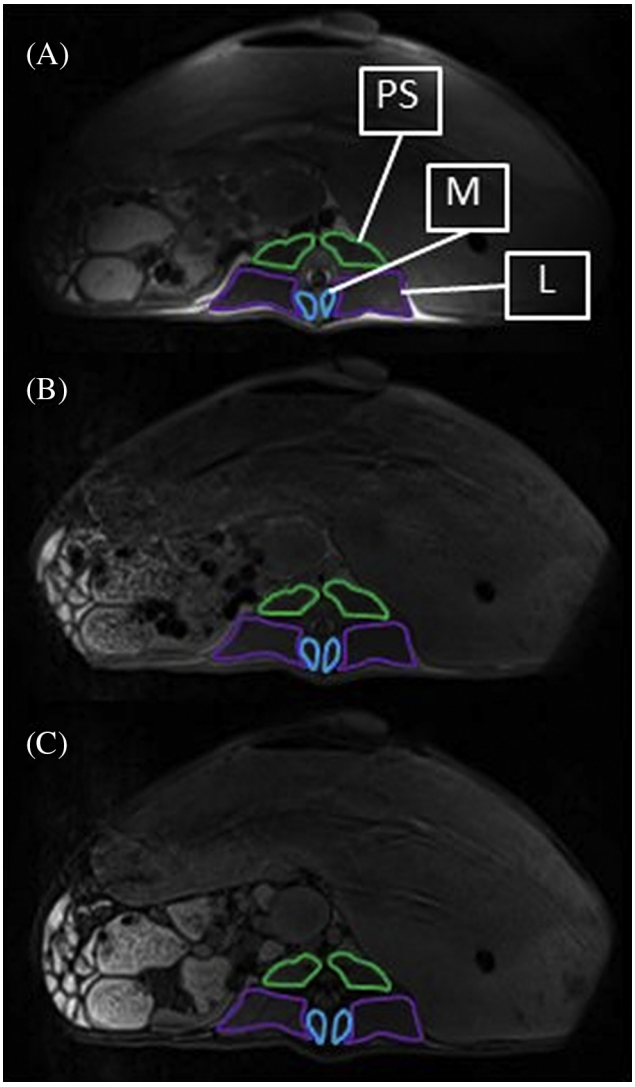

Figure 1 Region of interest of psoas major and minor (PS), multifidus (M), and longissimus (L) on both sides of L4 in (A) T1-weighted, (B) Dixon in-phase, and (C) Dixon oppose-phase axial images.

Statistical analysis

Statistical analysis was performed with SPSS (IBM, Armonk, NY: USA; version 22). The normal distribution of data was assessed using the Shapiro–Wilk test and by investigation of the frequency and Q–Q plots. For each muscle and spinal level, differences between MFI obtained from the intermuscular fat T1-weighted method, the subcutaneous fat T1-weighted method, and the Dixon method were evaluated using a one-way analysis of variance with *post hoc* Bonferroni correction or Friedman's analysis of variance with pairwise comparisons as the nonparametric equivalent. An independent *t* test or Mann–Whitney *U* test was

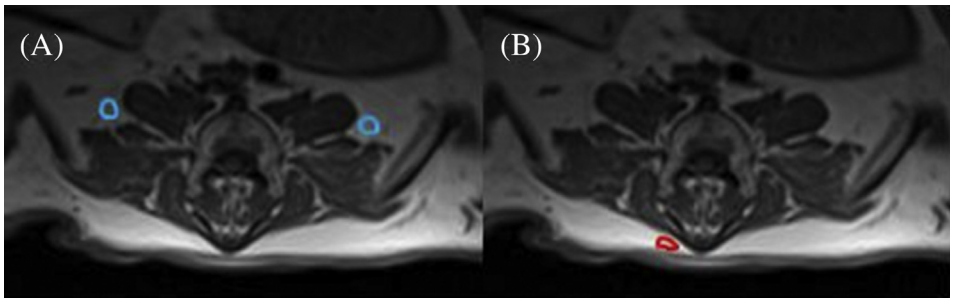

Figure 2 Region of interest of (A) intermuscular fat and (B) subcutaneous fat in an axial T1-weighted image at L6.

used to determine the significant differences between male and female sheep for each MFI quantification technique, muscle, and spinal level. To determine the intrarater reliability, an intraclass correlation ($ICC_{3,1}$) was performed on the first and second CSA ROI measures of all muscles and vertebral levels. Spearman's correlations were used to investigate the relationship between pathology grade and MFI, and between age and MFI for each MFI quantification technique, muscle, and spinal level.

Results

Out of the 17 sheep, three were excluded: two because of lack of measurable subcutaneous fat, and one because only a part Dixon sequence is available. Of the remaining 14 sheep, eight sheep were male. Mean age and body mass were 2.88 years (±3.06 years; range from 9 months to 8.5 years) and 66.75 kg (±20.34 kg), respectively. The majority of sheep ($n = 9$) had six lumbar vertebrae. No peri- or postanaesthesia complications occurred, and recovery was uneventful in all sheep except one, which required a tracheotomy after biting off parts of the intubation tube on sudden awakening after anaesthesia. Further treatment for this sheep consisted of daily wound cleaning, antibiotics, and anti-inflammatory agents (carprofen 1.5 mg/kg/d for 2 days and cefquinome 1 mg/kg/d for 2 days). Further recovery of this sheep was uneventful.

Intrarater reliability for ROI CSA of all muscles at all vertebral levels was high (ICC 0.930—0.997; Table 1). Table 2 shows the MFI values for the intermuscular fat T1-weighted method, the subcutaneous fat T1-weighted method, and the Dixon method. For all levels of all muscles, MFI determined using the subcutaneous fat T1-weighted method scored significantly lower than both the Dixon and intermuscular fat T1-weighted methods (all $p < 0.01$). For PS, the Dixon method produced significantly higher MFI than both the intermuscular and subcutaneous fat T1-weighted methods (all $p < 0.001$), although no significant differences were found between the Dixon method and the intermuscular fat T1-weighted method for any level of M and L. No significant differences were found between male and female sheep for any muscle, vertebral level, or MFI quantification method.

The pathology grade ranged from 0 to 2 (median 0.5). Seven sheep were evaluated as Grade 0, four sheep as Grade 1, and three sheep as Grade 2. The youngest sheep, which was assessed as Grade 2, was 3 years old. The correlations between MFI and age and MFI and pathology grade are shown in Tables 3 and 4, respectively.

Discussion

The presence of increased spinal muscle fat in patients with back and neck pain has been identified using MRI [4,5,7,10]. Even though the ovine is commonly used for experimental spinal investigations [19], ovine MFI had not been investigated using similar outcomes reported in humans. This study has quantified MFI in ovine lumbar spinal muscles using two different, but widely available, MRI techniques. The results showed that MFI outcomes from Dixon and T1-weighted sequences are comparable for the dorsal muscles M and L, if intermuscular fat—rather than subcutaneous fat—is used for T1-weighted images. In the human cervical spine, multifidus has also shown comparable muscle fat findings between T1-weighted and Dixon sequences

Table 1 Intrarater intraclass correlations (ICC) for the cross-sectional areas from the regions of interest of the muscles psoas major and minor (PS), multifidus (M), and longissimus (L) for L6 to L1.

Vertebra	Muscle	ICC	CI	
			Lower	Upper
L6	PS	0.982	0.943	0.994
	M	0.930	0.779	0.978
	L	0.985	0.953	0.995
L5	PS	0.992	0.975	0.998
	M	0.985	0.955	0.995
	L	0.997	0.988	0.999
L4	PS	0.997	0.988	0.999
	M	0.994	0.981	0.998
	L	0.996	0.984	0.999
L3	PS	0.997	0.992	0.999
	M	0.985	0.956	0.995
	L	0.997	0.991	0.999
L2	PS	0.991	0.973	0.997
	M	0.950	0.847	0.984
	L	0.996	0.970	0.999
L1	PS	0.985	0.952	0.995
	M	0.994	0.982	0.998
	L	0.996	0.982	0.999

CI = confidence intervals.

Table 2 Muscle fatty infiltrate (MFI) of psoas major and minor (PS), multifidus (M), and longissimus (L) for each vertebral level (L6—L1), obtained from T1-weighted sequences calculated relative to intermuscular fat (T1 int) and subcutaneous fat (T1 subcut), and from the Dixon sequences.

Muscle	Vertebra	T1 intermuscular MFI		T1 subcutaneous MFI		Dixon MFI	
		Mean (SD)	Median	Mean	Median	Mean	Median
PS	L6	37.65 (5.38)	37.15	22.38 (4.85)	22.83	56.40 (2.03)	55.94
	L5	35.79 (7.24)	35.25	21.05 (4.44)	19.46	54.86 (1.73)	54.60
	L4	31.85 (7.13)	31.00	18.63 (3.83)	17.55	54.43 (1.82)	54.16
	L3	30.15 (7.31)	30.95	17.55 (3.60)	17.98	53.97 (1.71)	53.99
	L2	31.58 (7.65)	32.06	18.58 (4.80)	19.17	54.29 (2.03)	54.08
	L1	34.08 (8.18)	36.32	20.14 (5.53)	19.85	56.19 (1.72)	56.52
M	L6	58.97 (12.55)	55.11[a]	34.67 (7.49)	32.58	58.03 (3.00)	56.84[a]
	L5	56.83 (14.62)	50.63[b]	33.18 (7.44)	30.57	57.41 (3.90)	56.29[b]
	L4	52.64 (13.18)[c]	48.61	30.81 (6.90)	29.25	55.98 (3.26)[c]	55.05
	L3	51.82 (13.35)[d]	47.50	30.14 (6.20)	28.35	55.83 (3.84)[d]	54.82
	L2	54.13 (13.90)[e]	47.27	31.57 (6.84)	29.90	55.91(3.81)[e]	55.05
	L1	55.54 (13.97)[f]	52.21	32.47 (7.23)	31.45	57.04 (4.41)[f]	56.02
L	L6	54.45 (12.88)	50.72[g]	31.81 (6.44)	30.46	57.67 (5.54)	55.64[g]
	L5	48.42 (8.61)	45.28[h]	28.67 (6.39)	26.85	51.93 (2.56)	50.97[h]
	L4	45.32 (8.09)	44.76[i]	26.88 (6.22)	26.17	51.31 (2.58)	50.23[i]
	L3	45.50 (9.64)	42.64[j]	26.57 (4.55)	25.56	51.20 (2.38)	50.16[j]
	L2	45.88 (9.18)	44.92[k]	27.13 (6.39)	26.79	51.15 (2.06)	50.33[k]
	L1	48.54 (7.80)	49.54[l]	28.96 (6.90)	29.73	51.32 (2.12)	50.73[l]

[a—l]Matching superscripts indicate nonsignificant differences between MFI quantification methods.
SD = standard deviation.

[16], where the mean signal intensity of C2 intermuscular fat was used. The reason why PS was significantly different between all methods compared in the present study whereas M and L were similar between the Dixon and T1-weighted intermuscular fat method, may be attributable to differences in muscle morphology such as fibre typing or internal structure complexity, although this would require further investigation using a histological approach. In T1-

Table 3 Correlations (corr) between age and muscle fatty infiltrate (MFI) using three different MFI quantification methods: T1 intermuscular, T1 subcutaneous, and Dixon.

Spinal level	Muscle	Correlations of MFI with age					
		T1 intermuscular		T1 subcutaneous		Dixon	
		corr (r)	p	corr (r)	p	corr (r)	p
L6	P	0.050	0.864	−0.607*	0.021	0.624*	0.017
	M	0.635*	0.015	−0.156	0.595	0.429	0.126
	L	0.853**	< 0.001	0.115	0.696	0.690**	0.006
L5	P	0.147	0.617	−0.610*	0.021	0.296	0.305
	M	0.612*	0.020	−0.021	0.944	0.472	0.088
	L	0.415	0.140	−0.410	0.145	0.481	0.082
L4	P	0.089	0.761	−0.633*	0.015	0.282	0.329
	M	0.328	0.252	−0.330	0.249	0.424	0.131
	L	0.216	0.459	−0.596*	0.024	0.608*	0.021
L3	P	0.151	0.606	−0.722**	0.004	0.388	0.171
	M	0.408	0.147	−0.183	0.530	0.268	0.354
	L	0.209	0.474	−0.596*	0.024	0.489	0.076
L2	P	−0.053	0.858	−0.706**	0.005	0.342	0.232
	M	0.374	0.188	−0.021	0.944	0.275	0.341
	L	0.131	0.656	−0.578*	0.030	0.731**	0.003
L1	P	−0.199	0.494	−0.713**	0.004	0.000	> 0.99
	M	0.305	0.289	−0.165	0.573	0.362	0.203
	L	−0.197	0.499	−0.702**	0.005	0.527	0.053

*$p < 0.05$.
**$p < 0.01$.

Table 4 Correlations (corr) between pathology grade and muscle fatty infiltrate (MFI) using three different MFI quantification methods: T1 intermuscular, T1 subcutaneous, and Dixon.

Spinal level	Muscle	Correlations of MFI with age					
		T1 intermuscular		T1 subcutaneous		Dixon	
		corr (*r*)	*p*	corr (*r*)	*p*	corr (*r*)	*p*
L6	P	−0.060	0.839	−0.593*	0.025	0.397	0.160
	M	0.444	0.111	−0.277	0.337	0.494	0.073
	L	0.702**	0.005	−0.043	0.884	0.573*	0.032
L5	P	0.060	0.839	−0.702**	0.005	0.253	0.382
	M	0.148	0.613	−0.425	0.130	0.444	0.111
	L	0.148	0.613	−0.552*	0.041	0.263	0.363
L4	P	0.201	0.491	−0.485	0.079	0.079	0.789
	M	0.210	0.471	−0.409	0.147	0.375	0.186
	L	0.306	0.288	−0.466	0.093	0.401	0.155
L3	P	0.158	0.590	−0.597*	0.024	0.229	0.430
	M	0.220	0.450	−0.327	0.253	0.375	0.186
	L	0.253	0.382	−0.440	0.116	0.306	0.287
L2	P	−0.189	0.518	−0.693**	0.006	0.229	0.430
	M	0.184	0.529	−0.320	0.264	0.392	0.166
	L	−0.007	0.981	−0.683**	0.007	0.640*	0.014
L1	P	−0.100	0.733	−0.518	0.058	−0.124	0.672
	M	0.299	0.300	−0.222	0.445	0.444	0.111
	L	−0.014	0.961	−0.545*	0.044	0.349	0.222

*$p < 0.05$.
**$p < 0.01$.

weighted images, fatty intramuscular septa are clearly identified, but smaller proportions of homogeneous intramuscular fat cannot be defined [26] and may even be invisible [13].

The subcutaneous fat T1-weighted method to determine MFI resulted in significantly lower MFI outcomes compared to the Dixon method for all muscles investigated. Although it is not known whether histological differences in fat composition exist between the intermuscular and subcutaneous fat locations used in the present study, it is most likely that the differences between methods found occurred because of B0 inhomogeneity, which can influence signal intensities in MRI [27] and is more pronounced further away from the isocentre of the magnet [28]. Furthermore, a gradient echo approach can experience smearing of signals from tissues with high fat content to adjacent musculature with low fat content, as it is sensitive to susceptibility effects [26]. These factors may also explain the differences seen in the present study for the correlations between MFI and pathology grade using the different MFI quantification methods. Both the intermuscular fat T1-weighted and Dixon method produced positive correlations with pathology grade and MFI, although the subcutaneous fat T1-weighted method produced only negative correlations. Previous studies have also shown positive associations in spinal pathology and muscle fat [29,30]. Therefore, using subcutaneous fat as a measure to determine MFI in sheep may not be appropriate based on the findings of the present study because of the potential limitations described above. Similarly, the negative associations found between age and MFI for the T1-weighted subcutaneous fat method should be interpreted with caution, because ageing has been reported to either have no influence on MFI of spinal muscles [29] or increased in some but not all spinal muscles [24]. For this reason, the negative correlations for the T1-weighted subcutaneous fat method should be interpreted with caution and the site of fat used to determine MFI in MRI studies should be considered carefully.

The quantification of MFI from MRI in the ovine lumbar spine has not been investigated; therefore, the results from the present study cannot be directly compared. However, based on near-infrared spectroscopy on samples of 100 g homogenous muscle after slaughter [31], thoracolumbar longissimus dorsi fat content in Merino cross-breed sheep has been determined [23,32]. The studies showed that intramuscular fat ranged from 3.82% to 4.84% across the breeds and age groups investigated. This is considerably lower than the findings from the present study, and this may be attributable to structural and fibre type differences between thoracic longissimus and the longissimus, or simply due to differences in breed and methodological approaches. To resolve this would require histological analyses.

CT is another imaging technique that can be used to identify fat content. In sheep carcasses, Gardner et al [33] used CT to determine whole carcass fat, although the fat content within muscle specifically was not reported. Others have investigated the relationship between muscle fat from infrared spectroscopy and pixel density on CT images from sheep carcasses [34], but only a moderate inverse correlation was found for the longissimus lumborum muscle. Lambe et al [35] obtained CT images in lambs *in vivo*, but this was also to determine internal fat rather than muscle

fat content. Further *in vivo* CT imaging of sheep carried out by these authors revealed that muscle density determined by Hounsfield units (HU) from CT was significantly associated with meat palatability [36]. This shows that CT may be a suitable tool for the assessment of fat content in muscle; however, the CT studies reported here used diverging HU boundaries for muscle and fat. Until it can be shown which fat and muscle HUs on CT correspond to muscle fat from histology, absolute sheep muscle fat determined from CT may be questionable. Furthermore, the boundary cutoffs for muscle, fat, and bone are influenced by the voltage used in CT acquisition [37]. The tube potential used in several sheep CT studies used higher values than that used in the present study.

In comparison to the existing literature on human spinal muscle MFI from multiple echo images, the apparently healthy ovine lumbar multifidus contains considerably more MFI. For example, multifidus MFI obtained from Dixon sequences in the present study ranged from 55% to 58% depending on vertebral level. On the contrary, cervical multifidus MFI from healthy human participants has been shown to range from 15% to 24% from Dixon sequences [16]. Direct comparisons to the human lumbar multifidus is limited because of the different methodological and analytical approaches used in other studies, for example, categorical MFI grading by visual inspection [4] or by reporting differences between in-phase and opposed-phase signal intensities [5,17]. No other studies were identified which investigated lumbar MFI in humans using multiecho images; however, by using ^{1}H proton MR spectroscopy, human lumbar multifidus was shown to contain 15% MFI in healthy participants and significantly greater MFI (24%) in patients with low back pain [3]. These values were reported as 26% and 29%, respectively, in the longissimus muscle. Therefore, spinal muscle MFI in healthy sheep appears to exceed that of MFI found in healthy participants and even in patients with back pain, based on MRI findings. The implications of these assumptions might suggest that a relatively smaller proportion of functional muscle tissue may be available in the ovine compared to man. This is less likely to be attributable to pathology and is probably attributable to the genetics underlying meat production, as intramuscular fat is a positive factor for meat palatability [32]. Fat proportion differences may, however, also have biomechanical implications, which at present have not been investigated in ovines *in vivo*. Muscle volume has been shown to have an influence on spinal stiffness *in vitro* [38]; however, a greater relative amount of fat in a given muscle volume may negatively influence muscle functionality [8].

Regardless of the differences between the human and sheep spine and spinal muscle morphology, sheep are commonly used as an animal model for the investigation of new spinal interventions prior to them being used in a clinical (human) population. Unfortunately, data from the ovine model are generally obtained *ex vivo*. This study has shown that MFI of the paraspinal muscles can successfully be determined from sheep *in vivo* using similar MRI acquisition methods as those used in humans. The benefits of future ovine model studies using such an approach are numerous. The paraspinal muscles are widely investigated in patients with low back pain; however, muscles in animal models have received very little attention, probably because of the *ex vivo* nature of animal model studies. Therefore, using the same MRI acquisition methods commonly used in humans for animal studies will allow comparable (*in vivo*) data to be obtained. This should provide a better insight into the possible changes in muscle tissue which may be seen as a result of spinal interventions tested preclinically. This would allow more rigorous testing and potentially provide better predictors on the clinical efficacy of interventions. Furthermore, careful recovery-based studies using animals can be utilised over several time points, which could provide for a better indicator of the clinical course of changes observed in paraspinal musculature.

There are several limitations in the present study which need to be acknowledged. First of all, for two out of the 14 sheep, sequences were obtained in a left to right phase direction because of the considerable movement artefacts seen in the anterior to posterior phase direction. This may have had an effect on signal intensity causing left to right side differences, but because the MPI of the two sides were taken, it was anticipated that this effect was minimal. In illustration, when the MFI data of all individual sheep for each vertebral level and muscle were ranked by increasing value, the mean rank of these two sheep were 7 out of 14 and 10 out of 14 for the T1-weighted images—placing them in the middle of the data set and not raising cause for concern. For the Dixon sequences, these findings were 2 and 5, respectively. Furthermore, because of the large proportion of rumen fluid to body tissues, movement artefacts were seen in most sheep although the quality of the images obtained was deemed sufficient for data analysis. Additionally, the Dixon approach is advantageous in cases where inhomogeneity artefacts may be a problem [39]. There was also a difference in slice thickness between the T1-weighted and Dixon sequences, and although this effect is thought to be minimal, caution is warranted when interpreting such data as they could contain partial volumes. Accordingly, image registration between T1 and Dixon images was not possible, but the multiecho Dixon images were coregistered. Attempts to coregister the T1 and Dixon images should be considered in future studies. In order to minimise bias, the single assessor in this study conducted the ROI twice with high intrarater reliability. Future studies should include multiple assessors of sheep muscle ROI to determine interrater reliability and enhance the robustness of the study findings. Previous work has shown acceptable interrater reliability of lumbar muscle ROI from T1-weighted MRI images in man, particularly for the muscles PS and L [40]; therefore, it is anticipated that similar reliability outcomes would be observed in sheep using these same MRI evaluation methods.

Future ovine studies should compare muscle fat findings obtained from MRI with fat values determined using muscle histology in the same sheep. Unfortunately, this approach was beyond the scope of the present study, and to our knowledge, a comparison of MRI- and histology-determined fat has, as yet, not been reported. However, this method has been carried out in a rabbit and pig model, which showed good agreement between MFI from Dixon sequences both at 1.5 T and 3.0 T and histology [15]. An additional aspect that should be quantified in similar future sheep studies is the composition of the fat (i.e., brown or

white adipose tissue) from the fat sample sites. A significant difference in signal intensity between brown and white fat has been shown in man using chemical shift water-fat MRI [41]; therefore, differences in the quantity of brown and white fat may be a possible source of error in muscle fat quantification. This may also explain the differences in muscle fat values calculated relative to intermuscular and subcutaneous fat. However, it has been shown that brown fat in sheep declines from birth, and at the age of 30 days, only white fat is discernible on histology of perirenal—abdominal adipose tissue [42]. Therefore, it is anticipated that this effect on signal intensity on the sheep in the present study is minimal.

Lastly, investigating different sheep breeds and sheep with higher grades of spinal pathology would also determine which sheep would be most suited to represent human muscle morphometric parameters of MFI and muscle volume. Gaining such information would be an important contribution to determining the appropriateness of the ovine as a human spinal model, as debate remains whether such animal models are appropriate in translational spinal research [43].

In conclusion, the Dixon multiecho fat/water sequence provides an acceptable comparison to T1-weighted sequences in the ovine lumbar multifidus and longissimus muscles if T1-weighted MFI is determined relative to intermuscular fat rather than subcutaneous fat. This is not the case for the psoas muscle, where both fat sources used to determine MFI from T1-weighted yielded significantly lower MFI values compared to the Dixon method. It was evident that the MRI-determined MFI of the ovine lumbar muscles found in this study is greater than the MFI in human lumbar muscles reported in the literature. This may have implications for sheep-to-human spine translational outcomes, because of the reduced biomechanical efficacy of muscle with increased MFI. Future studies should compare ovine MRI-obtained MFI with the gold standard biopsy.

Conflicts of interest

S.V., T.L., and A.E. have no conflicts of interest to declare. J.E. has 35% ownership in medical consulting start-up, Pain ID, LLC.

Funding/support

This study was financially supported by the Austrian Science Fund (FWF, project P24020).

References

[1] Samagh SP, Kramer EK, Melkus G, Laron D, Bodendorfer BM, Natsuhara K, et al. MRI quantification of fatty infiltration and muscle atrophy in a mouse model of rotator cuff tears. J Orthop Res 2013;31:421—6.
[2] Danneels LA, Vanderstraeten GG, Cambier DC, Witvrouw EE, De Cuyper HJ. CT imaging of trunk muscles in chronic low back pain patients and healthy control subjects. Eur Spine J 2000;9:266—72.
[3] Mengiardi B, Schmid MR, Boos N, Pfirmann CWA, Brunner F, Elfering A, et al. Fat content of lumbar paraspinal muscles in patients with chronic low back pain and in asymptomatic volunteers: quantification with MR spectroscopy. Radiology 2006;240:786—92.
[4] Kjaer P, Bendix T, Sorensen JS, Korsholm L, Leboeuf-Yde C. Are MRI-defined fat infiltrations in the multifidus muscles associated with low back pain? BMC Med 2007;5:2.
[5] Yanik B, Keyik B, Conkbayir I. Fatty degeneration of multifidus muscle in patients with chronic low back pain and in asymptomatic volunteers: quantification with chemical shift magnetic resonance imaging. Skel Radiol 2012;42:771—8.
[6] Hebert JJ, Kjaer P, Fritz JM, Walker BF. The relationship of lumbar multifidus muscle morphology to previous, current, and future low back pain: a 9-year population-based prospective cohort study. Spine 2014;39:1417—25.
[7] Elliott J, Jull G, Noteboom JT, Galloway G. MRI study of the cross-sectional area for the cervical extensor musculature in patients with persistent whiplash associated disorders (WAD). Man Ther 2008;13:258—65.
[8] Elliott JM, O'Leary S, Sterling M, Hendrikz J, Pedler A, Jull G. Magnetic resonance imaging findings of fatty infiltrate in the cervical flexors in chronic whiplash. Spine 2010;35:948—54.
[9] Elliott J, Pedler A, Kenardy J, Galloway G, Jull G, Sterling M. The temporal development of fatty infiltrates in the neck muscles following whiplash injury: an association with pain and posttraumatic stress. PLoS One 2011;6:e21194.
[10] Ulbrich E, Aeberhard R, Wetli S, Busato A, Boesch C, Zimmerman H, et al. Cervical muscle area measurements in whiplash patients: acute, 3, and 6 months of follow-up. J Magn Reson Imaging 2012;36:1413—20.
[11] Matsumoto M, Ichihara D, Okada E, Chiba K, Toyama Y, Fujiwara H, et al. Cross-sectional area of the posterior extensor muscles of the cervical spine in whiplash injury patients versus healthy volunteers — 10 year follow-up MR study. Injury 2012;43:912—6.
[12] Elliott JM, Galloway GJ, Jull GA, Noteboom JT, Centeno CJ, Gibbon WW. Magnetic resonance imaging analysis of the upper cervical spine extensor musculature in an asymptomatic cohort: an index of fat within muscle. Clin Radiol 2005;60:355—63.
[13] Reeder SB, Hu HH, Sirlin CB. Proton density fat-fraction: a standardized mr-based biomarker of tissue fat concentration. J Magn Reson Imaging 2012;36:1011—4.
[14] Gaeta M, Scribano E, Mileto A, Mazziotti S, Rodolico C, Toscano A, et al. Muscle fat fraction in neuromuscular disorders. Dual-Echo Dual-Flip-Angle spoiled gradient-recalled MR imagine techniques for quantification — a feasibility study. Radiology 2011;259:487—94.
[15] Smith AC, Parrish TB, Abbott R, Hoggarth MA, Mendoza K, Chen YF, et al. 1.5 Tesla and 3.0 Tesla versus histology. Muscle Nerve 2014;50:170—6.
[16] Elliott JM, Walton DM, Rademaker A, Parrish TB. Quantification of cervical spine muscle fat: a comparison between T1-weighted and multi-echo gradient echo imaging using a variable projection algorithm (VAPRO). BMC Med Imaging 2013;13:30.
[17] Paalanne N, Niinimäki J, Karppinen J, Taimela S, Mutanen P, Takatalo J, et al. Assessment of association between low back pain and paraspinal muscle atrophy using opposed-phase magnetic resonance imaging — a population-based study among young adults. Spine 2011;36:1961—8.
[18] Wilke H, Kettler A, Lutz CE. Are sheep spines a valid biomechanical model for human spines? Spine 1997;22:2365—74.
[19] Sheng SR, Wang XY, Xu HZ, Zhu GQ, Zhou YF. Anatomy of large animal spines and its comparison to the human spine: a systematic review. Eur Spine J 2010;19:46—56.
[20] Reitmaier S, Schmidt H, Ihler R, Kocak T, Graf N, Ignatius A, et al. Preliminary investigations on intradiscal pressures

during daily activities: an in vivo study using the Merino sheep. PLoS One 2013;8:369610.
[21] Reeves NP, Narendra KS, Cholewicki J. Spine stability: the six blind men and the elephant. Clin Biomech 2007;22:266—74.
[22] O'Leary S, Falla D, Elliott JM, Jull G. Muscle dysfunction in cervical spine pain: implications for assessment and management. J Orthop Sports Phys Ther 2009;39:324—33.
[23] McPhee MJ, Hopkins DL, Pethick DW. Intramuscular fat levels in sheep muscle during growth. Aust J Exp Agric 2008;48:904—9.
[24] Valentin S, Licka T, Elliott J. Age and side-related morphometric MRI evaluation of trunk muscles in people without back pain. Man Ther 2015;20:90—5.
[25] Carnier P, Gallo L, Sturaro E, Piccinini P, Bittante G. Prevalence of spondylosis deformans and estimates of genetic parameters for the degree of osteophytes development in Italian Boxer dogs. J Anim Sci 2004;82:85—92.
[26] Schick F, Machann J, Brechtel K, Strempfer A, Klumpp B, Stein D, et al. MRI of muscular fat. Magn Reson Med 2002;47:720—7.
[27] Wang J, Mao W, Qiu M, Smith MB, Constable T. Factors influencing flip angle mapping in MRI: RF pulse shape, slice-select gradients, off-resonance excitation, and B0 inhomogeneities. Magn Reson Med 2006;56:463—8.
[28] Dietrich O, Reiser MF, Schoenberg SO. Artefacts in 3-T MRI: physical background and reduction strategies. Eur J Radiol 2008;65:29—35.
[29] Fortin M, Yuan Y, Battié MC. Factors associated with paraspinal muscle asymmetry in size and composition in a general population sample of men. Phys Ther 2013;93:1540—50.
[30] Hyun SJ, Bae CW, Lee SH, Rhim SC. Fatty degeneration of paraspinal muscle in patients with the degenerative lumbar kyphosis: a new evaluation method of quantitative digital analysis using MRI and CT scan. J Spinal Disord Tech 2013. http://dx.doi.org/10.1097/BSD.0b013e3182aa28b0.
[31] Perry A, Shorthose WR, Ferguson DM, Thompson JM. Methods used in the CRC program for the determination of carcass yield and beef quality. Aust J Exp Agric 2001;41:953—7.
[32] Pannier L, Pethick DW, Geesink GH, Ball AJ, Jacob RH, Gardner GE. Intramuscular fat in the longissimus muscle is reduced in lambs from sires selected for leanness. Meat Sci 2014;96:1068—75.
[33] Gardner GE, Williams A, Siddell J, Ball AJ, Mortimer S, Jacob RH, et al. Using Australian Sheep Breeding Values to increase lean meat yield percentage. Anim Prod Sci 2010;50:1098—106.
[34] Anderson F, Pethick DW, Gardner GE. The correlation of intramuscular fat content between muscles of the lamb carcass and the use of computed tomography to predict intramuscular fat percentage in lambs. Animal 2015;9:1239—49.
[35] Lambe NR, Conington J, McLean KA, Navajas EA, Fisher AV, Buenger L. In vivo prediction of internal fat weight in Scottish Blackface lambs, using computer tomography. J Anim Breed Genet 2006;123:105—13.
[36] Lambe NR, Navajas EA, Fisher AV, Simm G, Roehe R, Buenger L. Prediction of lamb meat eating quality in two divergent breeds using various live animal and carcass measurements. Meat Sci 2009;83:366—75.
[37] Zurl B, Tiefling R, Winkler P, Kindl P, Kapp KS. Hounsfield units variations: impact on CT-density based conversion tables and their effects on dose distribution. Strahlenther Onkol 2014;190:88—93.
[38] Valentin S, Groesel M, Licka T. The presence of long spinal muscles increases stiffness and hysteresis of the caprine spine in-vitro. J Biomech 2012;45:2506—12.
[39] Brandao S, Seixas D, Ayres-Bato M, Castro S, Neto J, Marins C, et al. Comparing T1-weighted and T2-weighted three-point Dixon technique with conventional T1-weighted fat-saturation and short-tau inversion recovery (STIR) techniques for the study of the lumbar spine in a short-bore MRI machine. Clin Radiol 2013;68:e617—23.
[40] Valentin S, DeMott Yeates T, Licka T, Elliott J. Inter-rater reliability of trunk muscle morphometric analysis. J Back Musculoskelet Rehabil 2015;28:181—90.
[41] Hu HH, Perkins TG, Chia JM, Gilsanz V. Characterization of human brown adipose tissue by chemical-shift water-fat MRI. Am J Roentgenol 2013;200:177—83.
[42] Pope H, Budge H, Symonds S. The developmental transition of ovine adipose tissue through early life. Acta Physiol 2014;210:20—30.
[43] Alini M, Eisenstein SM, Ito K, Little C, Kettler AA, Masuda K, et al. Are animal models useful for studying human disc disorders/degeneration? Eur Spine J 2008;17:2—19.